Journal of the Energy Institute xxx (xxxx) xxx

Contents lists available at ScienceDirect

Journal of the Energy Institute

journal homepage: www.journals.elsevier.com/journal-of-the-energy-institute

Syngas preparation by NiO−$CaSO_4$-based oxygen carrier from chemical looping gasification technology

Jie Yang [a, b], Shengyu Liu [a, *], Liping Ma [b, **], Hongpan Liu [c], Jing Yang [b], Zhiying Guo [b], Ran Ao [b], Quxiu Dai [b]

[a] College of Resources and Environment, Chengdu University of Information Technology, Chengdu, Sichuan, 610225, China
[b] Faculty of Environmental Science and Engineering, Kunming University of Science and Technology, Kunming, Yunnan, 650093, China
[c] College of Chemistry and Environmental Engineering, Chongqing University of Arts and Sciences, Chongqing, 402160, China

ARTICLE INFO

Article history:
Received 20 February 2020
Received in revised form
28 August 2020
Accepted 6 September 2020
Available online xxx

Keywords:
Syngas production
Chemical looping gasification
NiO−$CaSO_4$-Based oxygen carrier

ABSTRACT

Phosphogypsum (PG) is a by-product in the phosphate fertilizer industry with high production. It is necessary to alleviate the problem of the storage pressing of PG. Nowadays, PG is applied as an oxygen carrier in lignite chemical looping gasification (CLG) in order to prepare syngas. In this process, the reaction temperature is usually above 1173 K, requiring much energy to reach this temperature. Here, the Ellingham diagram has used as a guide to finding the active phase of NiO combining with PG to prepare the NiO−$CaSO_4$ composite oxygen carrier. Using a variety of characterization techniques, it was found that in the oxygen carrier NiO−$CaSO_4$ with the waste-PG has a good dispersion of Ni specie. After analyzing the activity of the as-obtained oxygen carrier, it was demonstrated that the NiO−$CaSO_4$ could reduce the reaction temperature, resulting in reduced energy consumption. Notably, the oxygen carrier is essential for lignite conversion and CO and CO_2 production, especially for H_2 production. To promote the preparation of CO, the recommendable molar ratio of Ni element to PG is ≈ 1:1. As the number of cycles increases, agglomeration and cracks are occurring on the surface of the material. Based on these results, this work provides an oxygen carrier with the waste to reduce the reaction temperature for chemical looping and offer recommendations for future research.

1. Introduction

1.1. Syngas preparation

CO and H_2 are the main components of syngas, being widely applied as the starting material in various fields of chemical syntheses [1–6]. Although syngas can be obtained from coal or coke, and heavy oil or light hydrocarbons, the chemical looping gasification (CLG) can also be applied to produce syngas [6,7]. Based on preliminary results for the syngas production, CLG has the potential to achieve lower costs and higher power efficiencies than other technologies [8] with a net efficiency of around 41–42% [9–11].

1.2. CLG

In the process of CLG, where H_2 and CO are the main components, originating from the oxygen carrier reacting with the product of coal/biomass devolatilization/gasification [9]. Comparing the CLG process with the chemical looping combustion, the CLG can produce valuable combustible gases, having partial oxidation as the main reaction (R1). Additionally, steam and CO_2 is applied to enhance the reforming of steam (R2) and CO_2 (R3) for enhancing the production of syngas.

$$C_nH_{2m}O_p + (n-p)Me_xO_y \rightarrow nCO + mH_2 + (n-p)Me_xO_{y-1} \quad (R1)$$

$$C_nH_{2m}O_p + (n-p)H_2O \rightarrow nCO + (m+n-p)H_2 \quad (R2)$$

$$C_nH_{2m} + nCO_2 \rightarrow 2nCO + mH_2 \quad (R3)$$

For CLG, the oxygen carrier component is crucial. Nowadays,

* Corresponding author.
** Corresponding author.
E-mail addresses: shengyuliu_cuit@sina.com (S. Liu), LipingMaKMUST@163.com (L. Ma).

https://doi.org/10.1016/j.joei.2020.09.003
1743-9671/

many researchers are investigating CLG for metallic oxides, including Cu, Fe, Co, and Ni oxides and other compounds, such as $CaSO_4$ [13–16]. CuO is good at transferring oxygen in the lignite chemical looping gasification, which has been conformed by Dennis et al. [13]. Huang et al. applied the Fe-based material (natural iron ore) has been used as the oxygen carrier for CLG of biomass char, indicating that it is a good oxygen carrier candidate for char gasification [14]. Researchers found that the oxide of Mn, Co, Fe and Ni were used as oxygen carriers can promote carbon conversion in the process of chemical looping gasification [12,15,16]. $CaSO_4$-based materials are one of the most attractive oxygen carriers for industrial applications [17–19] due to their outstanding oxygen storage and release capability via the circular switching of $CaSO_4$/CaS redox couple [20–22]. Phosphogypsum (PG) is the by-product of the chemical industry in high amounts, low applicability, and seriously harmful to the environment [23,24]. And its main active ingredient is $CaSO_4$. Usually, an oxygen carrier consists of a mixture of substances that can provide better properties than its single component, such as the lattice oxygen reactivity, structural defects, and anti-sintering ability [9]. In order to improve the structure of the oxygen carrier, Cu, Fe, and Al has been combined to form the $Cu_{0.95}Fe_{1.05}AlO_4$ compound as an oxygen carrier [25]. At the same time, in other investigations, ZrO_2-supported Fe_2O_3–MnO_2 showed improved thermal stability and reaction performance for CLG [26]. In order to improve the performance of Mn-based oxygen carriers in CLG, several inert compounds have been used as their supporting material [9]. Jin et al. added several supports to improve the reactivity of Co-based oxygen carriers [27], while Yan et al. found that PG doped with a transitional element can reduce the thermal decomposition temperature of PG [28].

Most CLG tests have been carried out in the fluidized bed reactors (interconnecting fluidized bed, circulating fliuidized bed and so on) and fixed bed reactors (thermogravimetric analysis apparatus, tube furnace and so on). Each reactor has its own advantages. The fixed bed is easy to operate and the conversion rate of fluidized bed fuel is more higher. Researches were confirmed fluidized bed reactors can be applied to analyze thermochemical conversion because of their ability of near-constant temperatures and favourable mixing features [29]. Thermogravimetric analysis apparatus has been applied to analyze the char conversion [9]. To explore the thermodynamic and kinetic of lignite chemical looping gasification with CuO–$CaSO_4$ oxygen carrier, the tube furnace reactor has been used [2].

2. Objectives

In the previous studies, PG has been used as a single oxygen carrier to prepare syngas by CLG using lignite as the fuel [6,30], where the reaction temperature was ~1173 K, making this process uneconomic, even if in large-scale industrial productions, cost-efficiency is the leading and essential point to implement a chemical process. The main issue of CLG with PG is to lower the reaction temperature. In the investigations of Yan et al. [28], it was found that oxygen carrier, along PG can form an oxygen carrier, which can be an ideal candidate to solve this problem.

In the present study, using the Ellingham diagram, an oxygen carrier was found, preparing and characterizing the as-prepared material. To test its activity, the CLG experiments were carried out.

3. Experimental

For the present work, PG and lignite were purchased from Yunnan, China. And the composition of the material can be found in Table 1.

3.1. Oxygen carrier preparation

The oxygen carrier was prepared through the precipitation method, where nickel (II) nitrate hexahydrate ($Ni(NO_3)_2 \cdot 6H_2O$) was dissolved in deionized water, adding the PG (in the form of powder) slowly, in order to obtain a mixture with a different molar ratio of Ni and PG. Meanwhile, the pH of the mixed solution was adjusted to ≈8–9 using ammonia. Afterward, the samples were dried at 393 K overnight then placed into a muffle furnace to be calcined at 773 K for 300 min. The calcined materials were crushed, sieved, and stored in a desiccator, being labeled as NiO–$CaSO_4$.

3.2. Characterization

The dispersion of elements of the oxygen carrier was observed using an FEI Inspect S Scanning Electron Microscope-Energy Dispersive Spectrometer (SEM-EDS). The group of Ni in the oxygen carrier has been investigated by X-ray photoelectron spectroscopy (XPS) with a Thermo ESCALAB 250XI system and by Xplora Plus Ranman Microscope (Horiba Company, France). To analyze the crystal structure and the phase composition of NiO–$CaSO_4$, a Rigaku D/Max 2500 system with a Cu Kα radiation of X-ray diffraction (XRD) characterization has been used, with the scanning region of 5–90°.

3.3. Ellingham diagram

The Ellingham diagram showed the dependence of the stability of a substance on temperature, based on thermodynamics. The Gibbs free energy of the metal oxidation, corresponding to C and H, was plotted against temperature. From the view point of applicability, an ideal oxygen carrier in CLG should undergo multiple cycles of operation with a minimal loss in physical integrity and chemical reactivity. The redox potential of a metal oxide can be predicted using the Ellingham diagram [12,31], where the standard Gibbs free energy change of any reaction at any temperature can be calculated, and the suitable oxygen carrier can be found [29].

3.4. Experimental analysis

The performance of NiO–$CaSO_4$ oxygen carrier with lignite was evaluated using a KTL1600 tube furnace, using different molar ratios (NiO/$CaSO_4$: 0.25, 0.5, 1, 1.25, 1.5) with 80 mash at different temperatures from 873 K to 1073 K. During the experiments, nitrogen (99.999%) was used to remove air from the reactor in the

Table 1
Composition analyses of the material (wt.%).

PG	Composition	SO_3	CaO	SiO_2	total P_2O_5	hydrotropicP_2O_5	Al_2O_3	Fe_2O_3	MgO
	Content (%)	40.86	29.82	9.43	1.17	0.87	0.236	0.132	0.005
	Composition	total F	hydrotropic F	Na_2O	K_2O	MnO	free water	crystal water	Acid-insoluble
	Content (%)	0.52	0.12	0.043	0.086	0.002	5.38	4.27	8.42
Lignite	Composition	C	H	O	N	S	Moisture	Ash	Q_{net} (kJ/kg)
	Content (%)	62.47	4.36	30.73	1.35	1.09	25.7	6.54	17,820

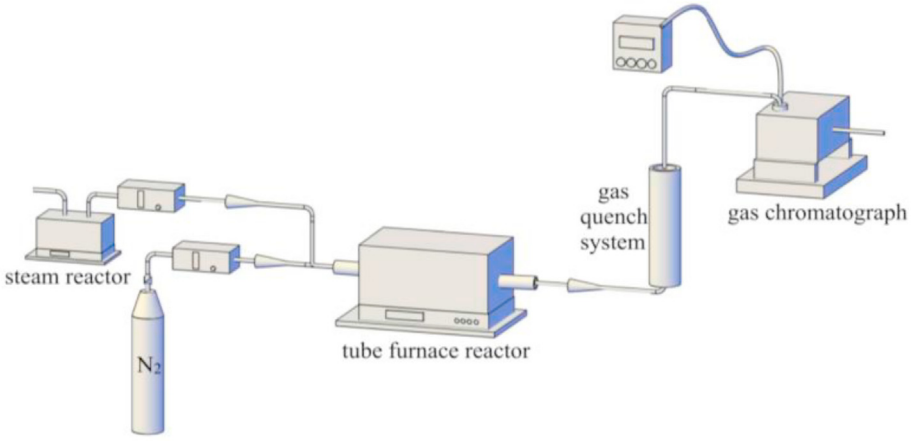

Fig. 1. Schematic diagram of CLG process.

first instance, then turned it on to be at 100 mL/min with water vapor. In this process, the carbon/steam ratio was around 1, and the oxygen carrier conversion was above 85% with the superior oxygen transfer capacity (0.46). The SP-2100A gas chromatograph was used to analyze the gaseous products (H_2, CH_4, CO, and CO_2). The construction of the experimental setup can be seen in Fig. 1.

The carbon of lignite conversion (*Xc* (%)): Xc is an important factor of lignite conversion, and it can be calculated using equation (1).

$$Xc = \frac{\sum(n_{co_2} + n_{CO} + n_{CH_4})}{\sum n_{c,\,fuel}} \times 100\% \quad (1)$$

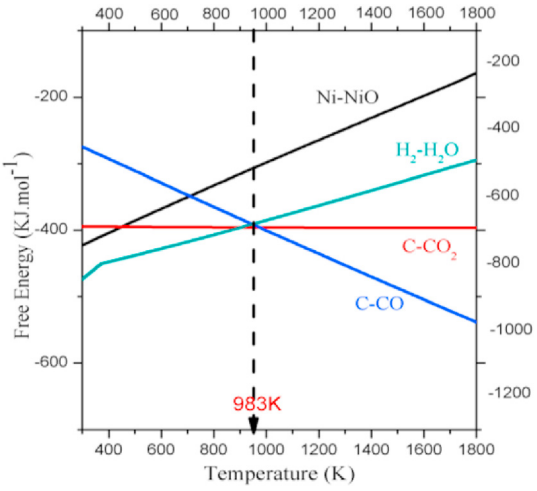

Fig. 2. Ellingham diagram for Ni, Mg, Ca, C and H.

where n_{CO2} (mol), n_{CO} (mol), n_{CH4} (mol), and $n_{c,\,fuel}$ (mol) refers to the molar quantity of CH_4, CO and CO_2, and the carbon in lignite, respectively.

Selective conversion of carbon (f_i (%)): f_i can be calculated using equation (2).

$$f_i = \frac{\sum n_i}{\sum(n_{CO2} + n_{CO} + n_{CH_4})} \times 100\% \quad (2)$$

where i could be CH_4, CO or CO.

The molar ratio of H_2: CO (H_2/CO): it is an essential factor characteristic of syngas, which can be calculated by equation (3).

$$H_2 \Big/ CO = \frac{\sum n_{H_2}}{\sum n_{CO}} \quad (3)$$

4. Results and discussion

4.1. Ellingham diagram

The reduction/oxidation potential of oxygen carriers can be predicted using the Ellingham diagram, which represents the standard Gibbs free energy of reactions as a function of temperature. Fig. 2 illustrates the Ellingham diagram for Ni, C, and H, demonstrating that C is easily oxidized to produce CO above 983 K, suggesting that higher temperature promotes the generation of CO. Besides, above 983 K, Ni–NiO line lies on the top of other lines, confirming NiO can be easily reduced by carbon, i.e., NiO can accelerate the decomposition of lignite. Thus, NiO has been intended to be the active phase in the oxygen carrier composite combined with PG.

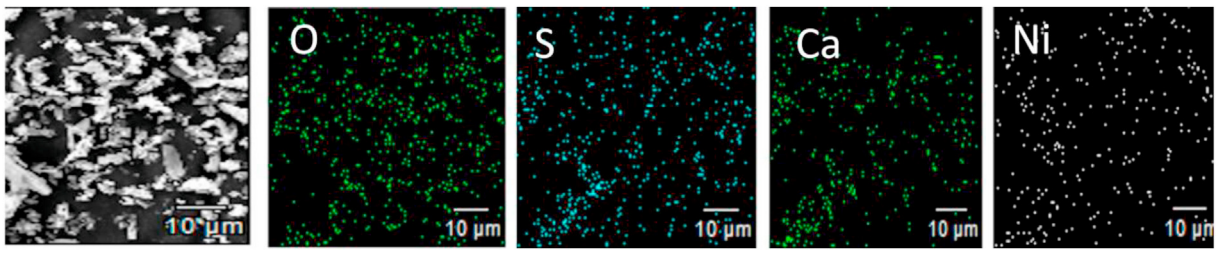

Fig. 3. SEM-EDS images of the compound oxygen carrier.

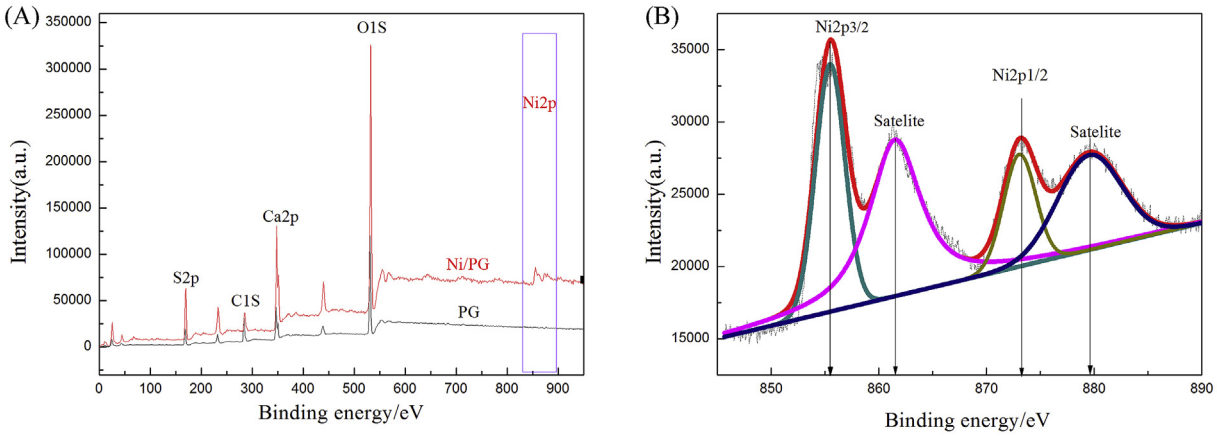

Fig. 4. XPS of (A) oxygen carriers; (B) Ni2p of NiO−$CaSO_4$.

4.2. Characterization

The SEM-EDS images of 1NiO−$CaSO_4$ oxygen carrier has analyzed. It can be seen from Fig. 3, the main elements of the oxygen carrier are well-distributed as the Ni component of the sample has an excellent dispersion. A high O, S, and Ca content also investigated in the oxygen carrier. The active elements of the oxygen carrier can be found, indicating the successful preparation of the NiO−$CaSO_4$.

The surface states of PG and NiO−$CaSO_4$ were investigated by XPS (see Fig. 4). The results have shown the presence of S, Ca, and O and the absent of Ni of PG. The phenomenon was following the previous results of Yan et al. [32]. The binding energy of Ni was observed when the Ni element was loaded to PG, as shown in Fig. 4 (A). In Fig. 4 (B), the Ni2p spectra of NiO−$CaSO_4$ samples are the characteristic of Ni^{2+} ions [33]. Thus, it was indicted that the NiO−$CaSO_4$ samples are containing Ni^{2+}.

Fig. 5 shows the XRD patterns of NiO−$CaSO_4$ oxygen carriers, sample Nos. (1)–(5) representing the 0.25NiO−$CaSO_4$, 0.5NiO−$CaSO_4$, 1NiO−$CaSO_4$, 1.25NiO−$CaSO_4$, and 1.5NiO−$CaSO_4$, respectively. $CaSO_4$ (the main peak appearing at $2\theta = 25.436°$) and SiO_2 ($2\theta = 20.859°$, 26.639°, and 59.958°) are the main ingredients along PG. The reflections at 37.441° and 43.472° are showing the presence of NiO. Additionally, the peak intensity of NiO increased as more Ni has been added to the oxygen carrier. Therefore, it was further conformed that the Ni exists in the form of bivalent in the composite oxygen carrier, which is the same as the result of XPS analysis.

The Raman spectrum of NiO−$CaSO_4$ oxygen carrier has been shown in Fig. 6, showing the characteristic peaks of NiO phase at 260–720 cm^{-1} [34,35]. Furthermore, the peaks from 500 to 650 cm^{-1} can be contributed to the Ni content. The intensity in the mixed oxide, which can be attributed to the presence of oxygen vacancies created in the phosphogypsum structure [36]. There is also a new peak of black NiO at 460 cm^{-1}. Mironova-Ulmane found the reason for the peak activation of the magnetostrictive effect at 450 cm^{-1}, which resulted in a slight rhomboidal deformation of NiO [37]. Besides, because of the symmetric and asymmetric stretching modes of sulfate anion (SO_4^{2-}), the peaks of $CaSO_4$ of PG appeared at 1008 and 1136 cm^{-1} [38].

In summary, NiO with a slight rhombohedral distortion were obtained during the synthesis of the oxygen carrier, with observable symmetric and asymmetric stretch modes of sulfate anion (SO_4^{2-}).

4.3. Reaction characteristics of the tube furnace

The effect of the amount of Ni in the NiO−$CaSO_4$ oxygen carrier was estimated. The CLG experiments were performed at the

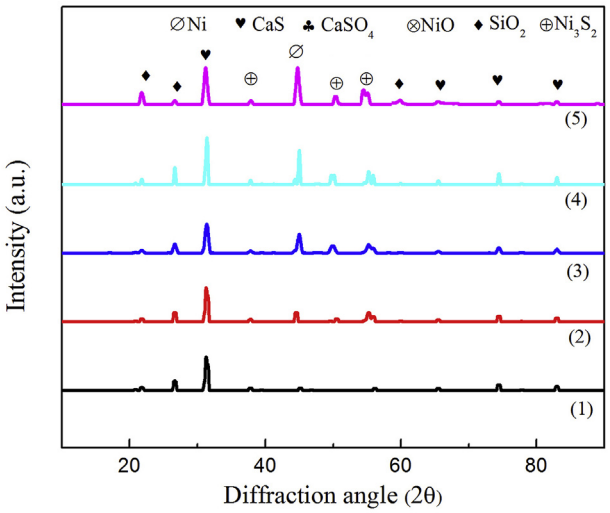

Fig. 5. XRD patterns of NiO−$CaSO_4$ oxygen carriers.

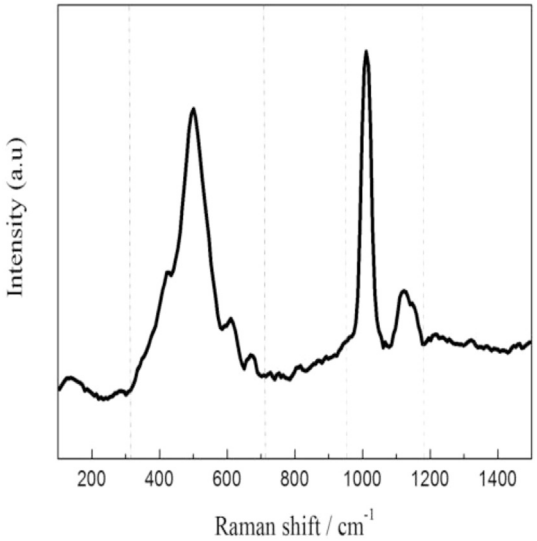

Fig. 6. Raman spectrum of NiO−$CaSO_4$.

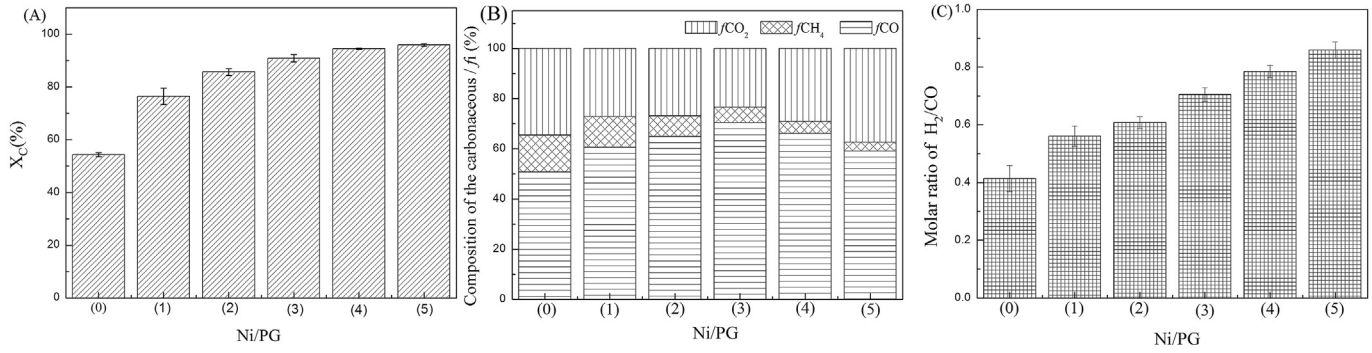

Fig. 7. Effect of NiO−$CaSO_4$: (A) *Xc*; (B) *fi*;(C) H_2/CO.

temperature of 1023 K under the steam atmosphere. Fig. 7 shows the carbon conversion, comparison of *f*CO, *f*CH_4, and *f*CO_2, the H_2/CO resulting from NiO−$CaSO_4$: (0) PG (1) 0.25NiO−$CaSO_4$, (2) 0.5NiO−$CaSO_4$, (3) 1NiO−$CaSO_4$, (4) 1.25NiO−$CaSO_4$, and (5) 1.5NiO−$CaSO_4$. As shown in Fig. 7(A), the carbon conversion increases with the increase of nickel content of the oxygen carrier. Besides, >95% carbon conversion was obtained as the molar ratio of Ni element to phosphogypsum was >1. The results indicated that the effect of the nickel content of NiO−$CaSO_4$ on the conversion of the carbon was significant. In the CLC systems with bituminous coal as fuel, the nickel-based oxygen carrier particles usually have good performance [39–41].

Furthermore, there is a high reactivity of Ni-based oxygen carriers when they are reacted with the products of the gasification process [42]. Therefore, in the case where Ni is present in the oxygen carrier NiO−$CaSO_4$, the fraction of CH_4 in the exhaust gas is lowered. However, the fraction of CO_2 decreased and then increased in the presence of Ni, is the opposite tendency for CO as shown in Fig. 7(B), i.e., CO was generated by the reaction of NiO−$CaSO_4$ with lignite. When there was a higher concentration of Ni, the reaction was promoted with CO to consume CO and to produce CO_2. Fig. 7(C) shows that the value of H_2/CO, in contrast, increased with the increasing of the nickel content. This indicates that a suitable amount of Ni can promote the generation of H_2, CO, and CO_2. Fig. 8 shows the reduced products of NiO−$CaSO_4$, where the main products are Ni, CaS, and Ni_3S_2. It can be concluded that NiO and $CaSO_4$, jointly promote the lignite gasification process. Based on the analyses above, the following reactions could occur.

$$CO_2 + H_2O(g) + 2CH_4 \rightarrow 3CO + 5H_2 \quad \text{(R4)}$$

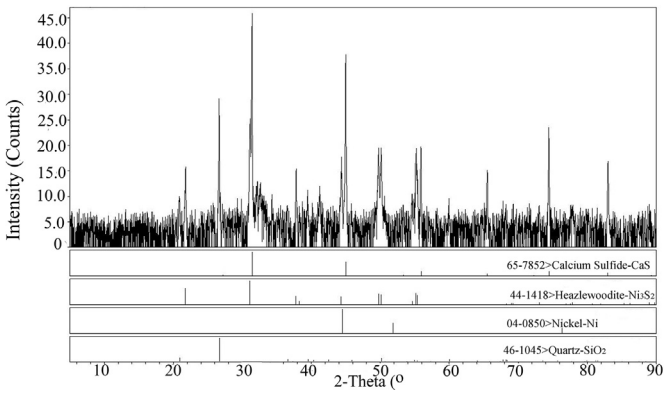

Fig. 8. The XRD of reduced NiO−$CaSO_4$.

$$NiO + CH_4 \rightarrow CO + 2H_2 + Ni \quad \text{(R5)}$$

$$CaSO_4 + 4C \rightarrow 4CO + CaS \quad \text{(R6)}$$

$$NiO + C \rightarrow CO + Ni \quad \text{(R7)}$$

$$NiO + CO \rightarrow CO_2 + Ni \quad \text{(R8)}$$

$$3Ni + 2H_2S \rightarrow Ni_3S_2 + 2H_2 \quad \text{(R9)}$$

As for CH_4 consumption and H_2 production, as shown in R5, NiO has been applied for CH_4 chemical-looping reforming [43]. Yang et al. also reported that phenomenon, where CO_2, vapor, and methane could be transformed to produce high amounts of CO [6,29]. Thus, R5 and R4 are the parallel competed reactions. Additionally, the primary reactions of CO generation are R6 and R7. The main reaction for the consumed CO can be found in R8 when more NiO exists. The oxygen carrier can fix the S element in the gas product via R9. Meanwhile, it would be poisoned and lost the active ingredient of Ni because of S element [12].

Based on the above analysis, it can be concluded that the Ni content of the oxygen carrier is essential for the conversion of carbon and the production of CO, CO_2, and H_2. For less CO consumed, the recommendable molar ratio of NiO vs. phosphogypsum is ~1:1.

Six reaction temperatures, from 873 K to 1073 K, have been selected to take under the loupe the influence of temperature on *Xc*, *fi* (*f*CO, *f*CH_4, and *f*CO_2), and H_2/CO using the 1NiO−$CaSO_4$ oxygen carrier. As can be observed in Fig. 9(A), the conversion rates of carbon at high reaction temperatures were higher than those at low temperatures. Thus, the higher temperature accelerates the reaction of the oxygen carrier and lignite (R6 and R7) [6,29], resulting in an increased yield of carbonaceous gas, especially for CO. On the other hand, higher temperatures eventually can decrease the generation of CO_2, as shown in Fig. 9(B). Inevitably, more hydrogen gases are formed in the gaseous product, because higher temperatures are promoting R4 and R5.

Therefore, it can be concluded that high temperature promotes the production of CO and H_2 production. Compared with only PG as the oxygen carrier in the previous work [6], the NiO−$CaSO_4$ oxygen carrier plays a well-defined role in CLG for syngas under lower temperatures. Thus, NiO−$CaSO_4$ decreases the reaction temperature of CLG for syngas generation, thus providing a cost-efficient approach.

Syngas also can be produced via coal or coke gasification and other ways. Most of the researchers are focusing on methods based on catalysts. For example, Vasconcelos et al. have prepared syngas with ruthenium- and platinum-based catalysts and the results

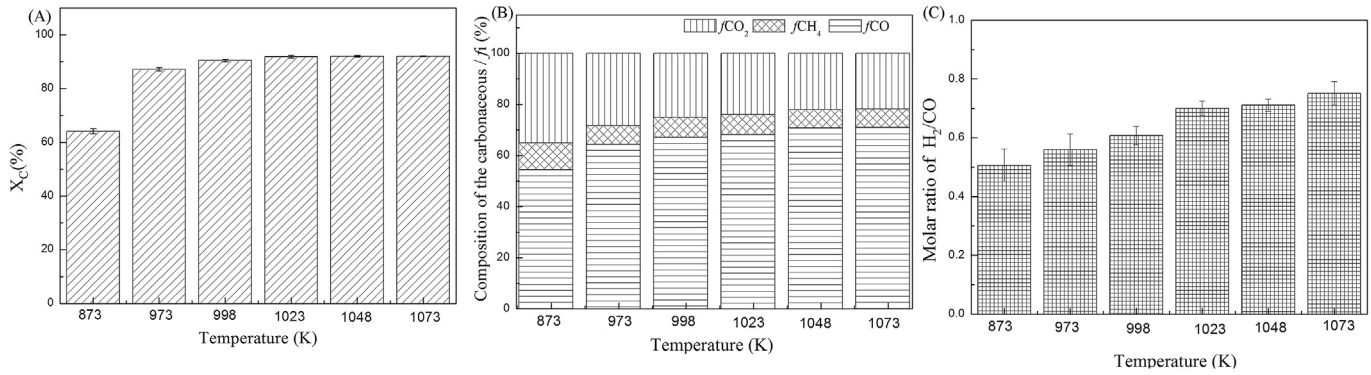

Fig. 9. Effect of temperature: (A) *Xc*; (B) *fi*;(C) H_2/CO.

showed that the conversion of CH_4 and CO_2 was around 50 and 67%, respectively [44]. Compared to the catalyst's pathway for syngas production, a higher conversion of raw materials can be achieved (the conversion of carbon of lignite is more than 90% in CLG above 1023 K). Compared to PG as an oxygen carrier, the NiO−$CaSO_4$ can lead to a stronger oxygen capacity of PG (high conversion of carbon of lignite can be achieved with smaller amounts of oxygen carrier). The higher reactivity of NiO can be presented (high conversion of carbon of lignite can be obtained at a lower temperature). On the other hand, the sulfur in the reaction gas can be captured by NiO, resulted in the poisoned of the oxygen carrier.

4.4. Microstructure changes of NiO−$CaSO_4$

The previous research showed that the recyclability of the oxygen carrier has an improved regeneration performance [6]. In order to further investigate the microstructure changes of NiO−$CaSO_4$ during the process of circulation, the microstructure of the oxygen carrier has been analyzed by SEM (see Fig. 10). The results found that as the number of cycles increases, agglomerations appeared on the surface of the material, and it was getting more and more fluffy. This can be attributed to the accumulation of ash.

5. Conclusion

A novel way is proposed to prepare NiO−$CaSO_4$ as oxygen carriers with the industrial waste-PG. The as-obtained material has shown improved characteristics such as it has a good dispersion of Ni specie. Besides, the added Ni covers the surface of PG, forming NiO with a slight rhombohedral distortion. Furthermore, a symmetric and an asymmetric stretch mode of sulfate anion (SO_4^{2-}) was observed in NiO−$CaSO_4$. Compared with PG as the oxygen carrier, the new oxygen carrier showed the advantageous character both of the PG and NiO (high oxygen capacity, high reactivity, and the improved sulfur capture capacity). It is also beneficial to CLG for syngas generation, reducing the reaction temperature. However, the oxygen carrier could be poisoned by the sulfur content during capture sulfur via $<3Ni + 2H_2S \rightarrow Ni_3S_2 + 2H_2>$, which is bad for the reuse of oxygen carrier.

Furthermore, the Ni of the oxygen carrier is significant for lignite conversion, CO, and CO_2 generation, especially for the H_2 generation. In order to get higher concentrations of CO, the

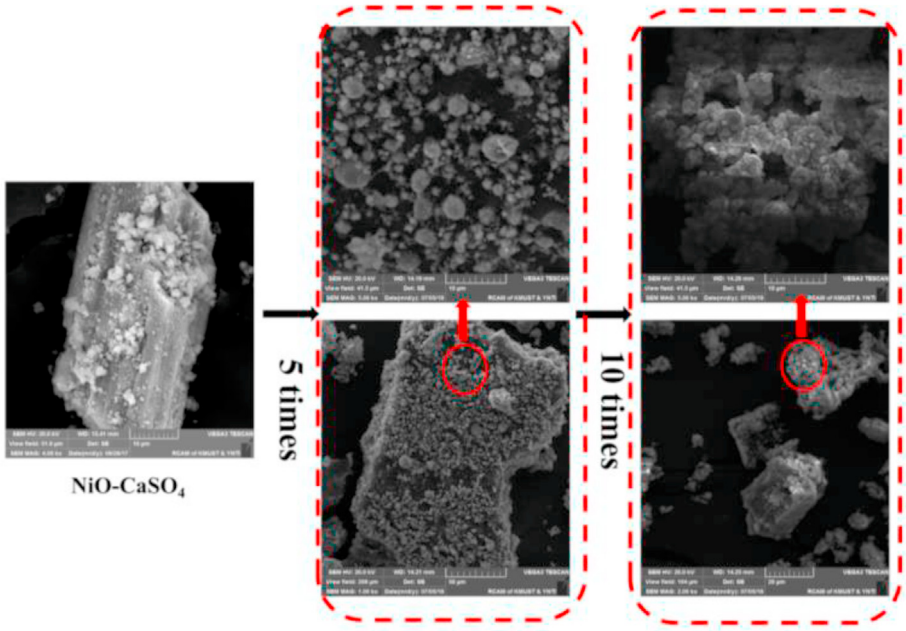

Fig. 10. SEM of recycled NiO−$CaSO_4$.

recommendable molar ratio of Ni to PG is ~1:1. As the number of cycles increases, agglomeration and cracks are occurring on the surface of the oxygen carrier.

Notes

The authors declare no competing financial interest.

Declaration of competing interest

The authors declare that they have no known competing financial interests or personal relationships that could have appeared to influence the work reported in this paper.

Acknowledgments

Financial supports for this project were provided by National Natural Science Foundation of China (No. 21676032 and No. 21666016), Key Research and Development Project Foundation of Science and Technology Department of Sichuan Province (No. 2020YFS0342) and the Foundation for High-level Talents of Chongqing University of Art and Sciences (No. 2017RCH07), which are greatly acknowledged.

Nomenclature

syn	molar of syngas generation (mol)
Xc	carbon conversion (%)
f_i	carbonaceous gases composition
n_i	molar of carbonaceous gases
i	i could be CO, CH_4 and H_2
f_{CH_4}	composition of CH_4 (%)
f_{co}	composition of CO (%)
f_{CO_2}	composition of CO_2 (%)
n_{CH_4}	molar of CH_4 (mol)
n_{co}	molar of CO (mol)
n_{CO_2}	molar of CO_2 (mol)
(0)	phosphogypsum
(1)	0.25NiO−$CaSO_4$
(2)	0.5NiO−$CaSO_4$
(3)	1NiO−$CaSO_4$
(4)	1.25NiO−$CaSO_4$
(5)	1.5NiO−$CaSO_4$

Abbreviations

PG	phosphogypsum
NiO−$CaSO_4$	oxygen carrier of Ni and phosphogypsum
CLG	Chemical Looping Gasification
XRD	X-ray diffraction
BET	Brunner-Emmet-Teller measurements
XPS	X-ray Photoelectron Spectroscopy
TGA	Thermogravimetric analyzer
SEM-EDS	Scanning Electron Microscope-Energy Dispersive Spectrometer

References

[1] H.M. Yu, Y. Liu, J.C. Liu, D.Z. Chen, High catalytic performance of an innovative Ni/magnesium slag catalyst for the syngas production and tar removal from biomass pyrolysis, Fuel 254 (2019). UNSP 115622.
[2] J. Yang, L.P. Ma, J. Yang, H.P. Liu, S.Y. Liu, Y.C. Yang, L.S. Mu, Y. Wei, R. Ao, Z.Y. Guo, Q.X. Dai, H.M. Wang, Thermodynamic and kinetic analysis of CuO-$CaSO_4$ oxygen carrier in chemical looping gasification, Energy 118 (2019). UNSP 116109.
[3] Z.W. Wang, K.G. Burra, T.Z. Lei, A.K. Gupta, Co-gasification characteristics of waste tire and pine bark mixtures in CO2 atmosphere, Fuel 257 (2019). UNSP 116025.
[4] D.W. Zeng, Y. Qiu, S. Peng, C. Chen, J.M. Zeng, S. Zhang, R. Xiao, Enhanced hydrogen production performance through the controllable redox exsolution within CoFeAlOx spinel oxygen carrier materials, J. Mater. Chem. 24 (6) (2018) 11306−11316.
[5] N. Chatrattanawet, S. Authayanun, D. Saebea, Y. Patcharavorachot, Syngas production from sugarcane leftover gasification integrated with absorption process for green liquid production, J. Clean. Prod. 235 (2019) 519−534.
[6] J. Yang, L. Ma, J. Tang, H. Liu, B. Zhu, Y. Lian, X. Cui, Chemical thermodynamics analysis for in-situ gasification chemical looping combustion of lignite with phosphogypsum for syngas, Appl. Therm. Eng. 112 (2017) 516−522.
[7] H. Ge, L. Shen, F. Feng, S. Jiang, Experiments on biomass gasification using chemical looping with nickel-based oxygen carrier in a 25 kWth reactor, Appl. Therm. Eng. 85 (2015) 52−60.
[8] C. Ekström, F. Schwendig, O. Biede, F. Franco, G. Haupt, G. de Koeijer, C. Papapavlou, P.E. Røkke, Techno-economic evaluations and benchmarking of pre-combustion CO_2 capture and oxy-fuel processes developed in the european ENCAP project, Energ Procedia 1 (2009) 4233−4240.
[9] J. Adanez, A. Abad, F. Garcia-Labiano, P. Gayan, L.F. de Diego, Progress in chemical-looping combustion and reforming technologies, Prog. Energy Combust. Sci. 38 (2012) 215−282.
[10] B. Fillman, M. Anheden, J. Wolf, Parameter study in order to reveal critical design issues in the design for a CLC power plant using solid carbon as fuel, in: Proc. 1st Int Conf on Chemical Looping, 2010. Lyon, France.
[11] F.X. Li, L.S. Fan, Clean coal conversion processes − progress and challenges, Energy Environ. Sci. 2 (1) (2008) 248−267.
[12] X. Zhao, H. Zhou, V.S. Sikarwar, M. Zhao, A.H.A. Park, P.S. Fennell, L. Shen, L.S. Fan, Biomass-based chemical looping technologies: the good, the bad and the future, Energy Environ. Sci. 9 (10) (2017) 1885−1910.
[13] Z. Huang, Y. Zhang, J.J. Fu, L.H. Yu, M. Chen, S. Liu, F. He, D.Z. Chen, G.Q. Wei, K. Zhao, A.Q. Zheng, Z.L. Zhao, H.B. Li, Chemical looping gasification of biomass char using iron ore as an oxygen carrier, Int. J. Hydrogen Energy 41 (2016) 17871−17883.
[14] J.S. Dennis, S.A. Scott, In situ gasification of a lignite coal and CO_2 separation using chemical looping with a Cu-based oxygen carrier, Fuel 89 (2020) 1623−1640.
[15] Z. Kun, D. He, J. Guan, L. Shan, Z. Wu, Q.M. Zhang, Coal gasification using chemical looping with varied metal oxides as oxygen carriers, Int. J. Hydrogen Energy 45 (2020) 10696−10708.
[16] Y. Qiu, L. Ma, D.W. Zeng, M. Li, D.X. Cui, Y.L. Lv, S.A. Zhang, R. Xiao, Efficient CO_2 to CO conversion at moderate temperatures enabled by the cobalt and copper co-doped ferrite oxygen carrier, J Energy Chem 46 (2020) 123−132.
[17] J. Yang, L.P. Ma, J. Yang, Z.Y. Guo, H.P. Liu, W. Zhang, Chemical looping gasification of phosphogypsum as an oxygen carrier: the Ca and S migration mechanism using the DFT method, Sci. Total Environ. 689 (2019) 854−864.
[18] B. Wei, H. Tan, Y. Wang, X. Wang, T. Yang, R. Ruan, Investigation of characteristics and formation mechanisms of deposits on different positions in full-scale boiler burning high alkali coal, Appl. Therm. Eng. 119 (2017) 449−458.
[19] H. Fu, J. Huang, L. Yin, J. Yu, W. Lou, G. Jiang, Retarding effect of impurities on the transformation kinetics of FGD gypsum to a-calcium sulfate hemihydrate under atmospheric and hydrothermal conditions, Fuel 203 (2017) 445−451.
[20] M. Zheng, Y.B. Xing, K.Z. Li, S.M. Zhong, H. Wang, B.L. Zhao, Enhanced performance of chemical looping combustion of CO with CaSO4-CaO oxygen carrier, Energy Fuel. 31 (5) (2017) 5255−5265.
[21] R. Xiao, Q.L. Song, Characterization and kinetics of reduction of CaSO4 with carbon monoxide for chemical-looping combustion, Combust. Flame 158 (12) (2011) 2524−2539.
[22] X. Jia, Q.H. Wang, K.F. Cen, L.M. Chen, An experimental study of CaSO4 decomposition during coal pyrolysis, Fuel 163 (2016) 157−165.
[23] Q. Che, Q. Zhang, A. Fourie, C. Xin, Utilization of phosphogypsum and phosphate tailings for cemented paste backfill, J. Environ. Manag. 201 (2017) 19−27.
[24] M. Francisco, R.C. Carlos, C.H. Pablo, C. Sergio, P.A. Maria, M.N. José, P.L. Rafael, An anomalous metal-rich phosphogypsum: characterization and classification according to international regulations, J. Hazard Mater. 331 (2017) 99−108.
[25] S. Rifflart, A. Lambert, A. Delebarre, J. Salmi, B. Durand, S. Carpentier, CLCMAT project- material development for "chemical looping combustion, in: Proc 1st Int Conf on Chemical Looping, 2010. Lyon, France.
[26] E. Ksepko, R.V. Siriwardane, H. Tian, T. Simonyi, J.A. Poston, A. Zinn, M. Sciazko, Effect of H_2S on chemical looping combustion of coal derived synthesis gas over Fe_2O_3-MnO_2 supported on ZrO_2/sepiolite, in: Proc. 1st Int Conf on Chemical Looping, 2010. Lyon, France.
[27] H. Jin, T. Okamoto, M. Ishida, Development of a novel chemical-looping combustion: synthesis of a looping material with a double metal oxide of CoO-NiO, Energy Fuel. 12 (1998) 1272−1277.
[28] B. Yan, L. Ma, L. Xie, J. Ma, Z. Zi, X. Yan, Reaction mechanism for iron catalyst in the process of phosphogypsum decomposition, Ind. Eng. Chem. Res. 52 (2013) 17383−17389.
[29] S. Iannello, S. Morrin, M. Materazzi, Fluidised bed reactors for the thermochemical conversion of biomass and waste, Kona powder Part. J 37 (2020) 114−131.
[30] J. Yang, L. Ma, S. Dong, H. Liu, S. Zhao, X. Cui, D. Zheng, J. Yang, Theoretical and experimental demonstration of lignite chemical looping gasification of phosphogypsum oxygen carrier for syngas generation, Fuel 194 (2017) 448−459.
[31] H.E. Bartlftt, K.E. Johnson, Electrolytic reduction and Ellingham diagrams for oxy-anion systems, Can. J. Chem. 44 (18) (1966) 2119−2129.

[32] B. Yan, L. Ma, J. Ma, Z. Zi, X. Yan, Mechanism analysis of Ca, S transformation in phosphogypsum decomposition with Fe catalyst, Ind. Eng. Chem. Res. 53 (2014) 7648–7654.
[33] N.V. Kosova, E.T. Devyatkina, V.V. Kaichev, Optimization of Ni^{2+}/Ni^{3+} ratio in layered Li(Ni,Mn,Co)O_2 cathodes for better electrochemistry, J. Power Sources 174 (2007) 965–969.
[34] R.E. Dietz, G.I. Parisot, A.E. Meixner, Infrared absorption and Raman scattering by two-magnon processes in NiO, J. Appl. Phys. 42 (1971) 2302–2310.
[35] J.C. Lai, X.C. Wang, W.B. Mi, Y.H. Ding, B.H. Yang, Structure and optical properties of polycrystalline NiO films and its resistive switching behavior in Au/NiO/Pt structures, Physica B 478 (2015) 89–94.
[36] C.A. Chagas, E.F. de Souza, R.L. Manfro, S.M. Landi, M.M. Souza, M. Schmal, Copper as promoter of the NiO–CeO_2 catalyst in the preferential CO oxidation, Appl. Catal. B Environ. 182 (2016) 257–265.
[37] N. Mironova-Ulmane, A. Kuzmin, I. Steins, J. Grabis, I. Sildos, Raman scattering in nanosized nickel oxide NiO, J. Phys. Conf. 93 (2007), 012039.
[38] S.J. Brotton, R.I. Kaiser, In situ Raman spectroscopic study of gypsum (CaSO4·2H2O) and epsomite (MgSO4·7H2O) dehydration utilizing an ultrasonic levitator, J. Phys. Chem. Lett. 4 (2013) 669–673.
[39] G.T. Tyuliev, K.L. Kostov, XPS/HREELS study of NiO films grown on Ni(111), Phys. Rev. B 60 (1999) 2900–2907.
[40] M.W. Roberts, R.S.C. Smart, The defect structure of nickel oxide surfaces as revealed by photoelectron spectroscopy, J. Chem. Soc. Faraday. Trans. 80 (1984), 29571-2968.
[41] I. Ahmed, H. de Lasa, 110th Anniversary: kinetic model for syngas chemical looping combustion using a Nickel-based highly performing fluidizable oxygen carrier, Energy Fuel. 33 (9) (2019) 9149–9160.
[42] J. Yang, L. Ma, J. Yang, H. Xiang, H. Liu, Z. Guo, Mechanism of lignite-to-pure syngas low temperature chemical looping gasification synergistic in situ S capture, Fuel 222 (2018) 675–686.
[43] Han Lu, Z. Zhou, M.B. George, Model-based analysis of chemical-looping combustion experiments. Part II: optimal design of CH4-NiO reduction experiments, AIChE J. 62 (2016) 2432–2446.
[44] B.D. Vasconcelos, L. Zhao, P. Sharrock, A. Nzihou, D.P. Minh, Catalytic transformation of carbon dioxide and methane into syngas over ruthenium and platinum supported hydroxyapatites, Appl. Surf. Sci. 390 (2016) 141–156.